The physical characteristics of hypersonic flows

J. Urzay
Center for Turbulence Research, Stanford University, Stanford CA 94305

July 2020

Hypersonics is the field of study of a very particular class of flows that develop around aerodynamic bodies moving in gases at exceedingly high velocities compared to the speed of the sound waves. The description of the gas environment surrounding a hypersonic vehicle is important for the calculation of thermomechanical loads on the body. These notes provide a qualitative characterization of hypersonic flows in terms of characteristic scales encountered in engineering applications. The wealth and peculiarity of the gasdynamic phenomenology emerging around hypersonic flight systems is summarized schematically in Fig. 1 and elaborated in the remainder of these notes.

1. The hypersonic range of Mach numbers

In most practical applications related to Hypersonics, the velocities associated with aircrafts and spacecrafts piercing through the terrestrial atmosphere are within the range $U_\infty \sim 1.7-12.6$ km/s (i.e., approximately $5-42$ kft/s, $6,000-45,000$ km/h, or $3,800-28,000$ mph). This range of velocities approximately translate into flight Mach numbers $5 \lesssim Ma_\infty \lesssim 42$ in the stratospheric and mesospheric layers of the terrestrial atmosphere, with Ma_∞ being defined as

$$Ma_\infty = U_\infty/a_\infty \tag{1}$$

based on the speed of the sound waves in the free stream a_∞. The lower end of this interval corresponds to applications of low-altitude high-speed flight and impact of warheads on ground targets, whereas the upper end represents conditions approached by spacecrafts re-entering the terrestrial atmosphere while returning from the Moon, Mars or Venus.

It is indisputable that the velocities mentioned above can be classified within the realm of what is colloquially understood as *"very fast"* compared to ordinary velocities observed

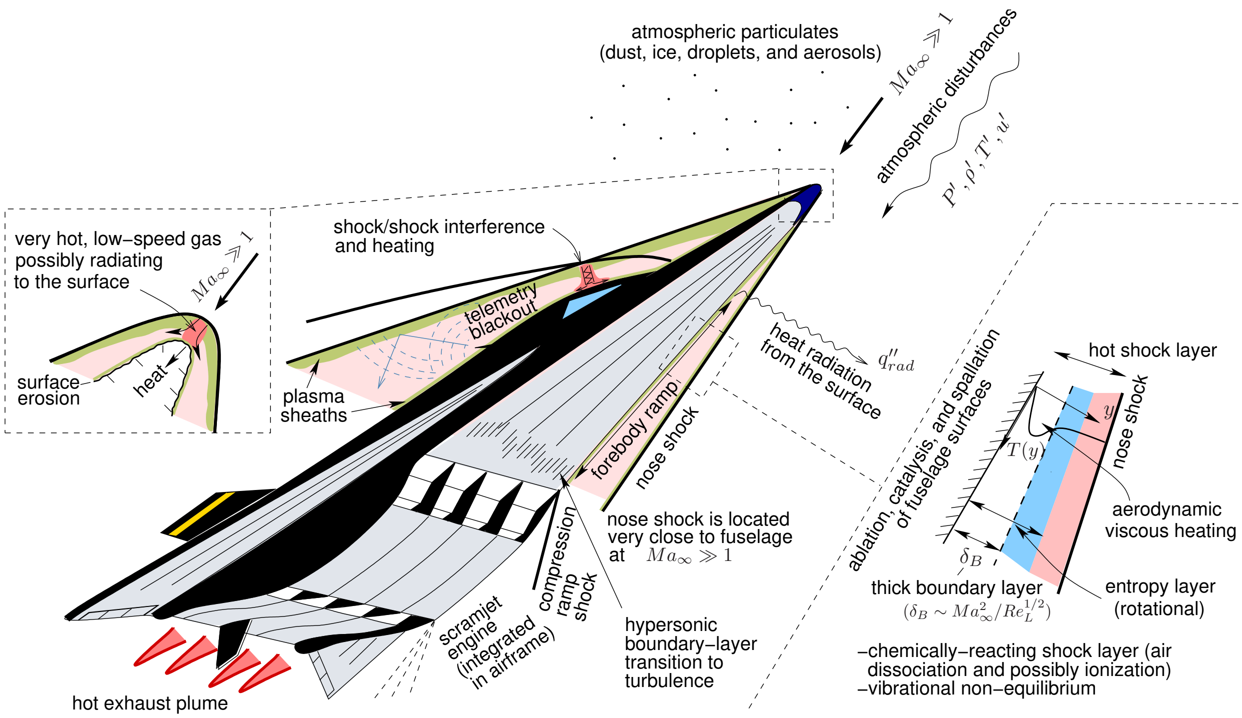

Figure 1: Gasdynamic phenomenology around a notional hypersonic flight system.

in physical processes or engineering applications in everyday life. For instance, an object moving at Mach 10 travels a distance of approximately 3.4 km (i.e., 30 football fields) every second. This is very fast compared to the 27 m we drive every second in a highway at 100 km/h with a car, or to the 250 m traveled every second by an airliner during cruse flight at Mach 0.8. While the airliner needs more than 10 hrs to fly a distance equivalent from San Francisco straight to Madrid, the same distance could be traversed in 45 mins by a hypersonic flight system at Mach 10. Such system would turn around the world flying along the equator in less than 4 hrs.

However enticing these futuristic tales of high-speed aviation may sound, a number of unsolved technical issues arise when imparting such high velocities to any flight system. Some of these problems are related to hypersonic aerothermodynamics and pertain to the main subject of these notes, whereas others are connected instead with flight mechanics. Consider, for instance, an event during flight requiring the pilot or the guidance computer to execute a course correction. An airliner travels approximately 50 m during the 0.2 s of typical pilot reaction time, whereas an aircraft flying at Mach 10 would cover 700 m during that same time. In practice, these distances are much longer because of the lag introduced by the mechanisms responsible for actuating the control surfaces, and therefore the aircraft at Mach 10 would need more than a couple of kilometers of safe airspace from the time the pilot commits to take action to the time the control surfaces have started moving. These are impractical distances in combat situations where the action taken is aimed at firing weapons at enemy planes, or in scenarios when a spatially compact maneuver is required to dodge an incoming missile or to avoid fatal crash.

The flyer of hypersonic planes must not only have a very short reaction time to minimize these lag distances, but must also be capable of withstanding very large accelerations. For example, to keep horizontal accelerations in the cockpit below the maximum tolerable limit of 8 g's, above which the performance of combat pilots is greatly reduced, a 90°-turn performed at Mach 10 would require a total maneuver time longer than 30 s over a trajectory with curvature radius larger than 150 km, similar to the size of the state of Maryland. Untrained passengers, whose maximum acceptable limits of acceleration are much lower than those of a combat pilot, would undoubtedly prefer the comfort of a conventional airliner.

Technological progress over the last 70 years have now made the conventional airliner a routinary and safe means of transporting more than 200 passengers at once across continents. In contrast, little to nothing has been established about the airworthiness certifications that a hypersonic airliner would have to meet. An aspect that would perhaps have to be accounted for would be the disconcerting amount of inertia that a hypothetical hypersonic airliner weighing 200,000 kg, similar to a fully loaded Boeing 777, would have in flight. Had this hypersonic airliner have a crash accident due to unfortunate circumstances, its kinetic energy at Mach 5 would be equivalent to 70 tons of TNT, or 7 times the explosive yield of the GBU-43/B MOAB – the most advanced thermobaric weapon available.

Setting these practical issues momentarily aside, and focusing back on the fluid-mechanical aspects sketched in Fig. 1, the specific reasons that justify dubbing the aforementioned range of Mach numbers as *"hypersonic"* in a technical sense, as to imply a completely different character relative to supersonic velocities, stem from the emergence of the following physical characteristics in the resulting flow field:

(a) *the high temperatures prevailing in the post-shock gases,*

(b) *the short residence times of the gas molecules around the flight system,*

(c) *the high rates of aerodynamic heating of the fuselage,*

(d) *the absence of linearity in the inviscid slender-body limit.*

These aspects represent cornerstones that fundamentally separate hypersonic from supersonic flows.

Flows over bodies at $Ma_\infty \gtrsim 5$ lead to significant departures from calorically perfect behavior in the surrounding gas. These departures are induced by the resulting high temperatures in the gas behind the shock waves generated by the fuselage. For a fixed body geometry, the first of these phenomena to appear as the velocity is increased is the vibrational excitation of the gas molecules, but the onset is rather gradual and starts to become noticeable at approximately 800 K in air. Note that the temperature behind a normal shock in stratospheric air at $Ma_\infty = 5$ is approximately $1,300$ K. As a result, other than yielding post-shock temperatures in the right ballpark for significant activation of the vibrational degrees of freedom of the molecules, there is nothing extraordinary that can be adjudicated to the threshold $Ma_\infty = 5$. The lower end of the hypersonic range of Mach numbers may be completely different in contrived or extraterrestrial atmospheres formed by gases very different from air and whose non-calorically-perfect behavior may begin at much lower or much higher temperatures. Additional processes observed as the velocity is increased involve chemical conversion, including dissociation and ionization of the gas molecules, along with thermal radiation from solid surfaces and from the bulk of the gas volume. In practical applications, some of these processes may interact with the fuselage or thermal shield, thereby leading to complex coupled dynamics. To compound the problem, many of these processes develop under chemical and thermodynamic non-equilibrium because of the relatively short residence time of the gas molecules around the hypersonic flight system, in that the rates of collisions between gas molecules are not large enough to establish equilibrium.

An important consequence of the prevailing high temperatures is the high rates of heating of the fuselage. The generation of such large heating rates is due to compressibility mechanisms whereby thermal energy is aerodynamically recovered through transformation of kinetic energy. This excess of thermal energy can be conducted or radiated as heat. It is for this reason that the phenomenon was named *"aerodynamic heating"* [1]. It proves counter-intuitive even for researchers trained in Fluid Mechanics, since strong aerodynamic heating of the fuselage can occur even if its temperature is comparable or larger than the static temperature of the gas in the free stream overriding the fuselage. The structural damage of the fuselage caused by aerodynamic heating is perhaps the most important culprit of Hypersonics and leads to a never-ending *"heat barrier"*, whose imaginary height increases indefinitely with increasing Mach numbers above 5, as opposed to the clearly delineated *"sound barrier"* acting only at Mach 1.

While the physical characteristics mentioned above are related to complex thermochemical effects induced by the high speeds and the hot temperatures they engender, there is an important defining aspect of Hypersonics that is observed even in cold flows and finds justification on simper grounds. In the history timeline of the development of Hypersonics, much of the early work was focused on solving the problem of inviscid flows of calorically perfect gases at high Mach numbers over slender bodies such as ogives and cones. A small-disturbance theory already existed for describing supersonic flows over slender bodies, which was linear because of the vanishing strength of the shocks emanating from the body surface, whose local inclination angle $\delta \ll 1$ is always much smaller than the Mach angle at supersonic

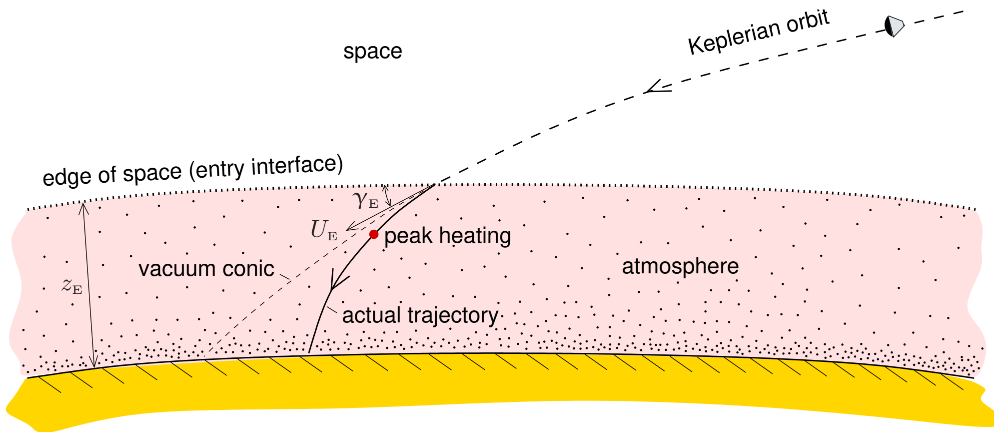

Figure 2: Schematics of atmospheric re-entry.

Mach numbers (i.e., $Ma_\infty \delta \ll 1$). In contrast, the counterpart theory for hypersonic flows, first derived by Tsien [2], necessarily required retaining nonlinear terms. The root cause of these nonlinearities is the large strength of the shock waves induced by the body surface at hypersonic Mach numbers, whose local inclination angle is of the same order or larger than the Mach angle (i.e., $Ma_\infty \delta \gtrsim 1$), which results in supersonic velocity disturbances normal to the free stream. These nonlinearities fundamentally affect the flow and hinder the derivation of closed forms for drag and lift coefficients, which back in the years when the inviscid theory was at the forefront of research, motivated extensive work on hypersonic-similarity rules for the design of hypersonic flight systems [3].

2. Hypersonic velocity scales for re-entry

A prominent application of Hypersonics is the re-entry of spacecrafts in planetary atmospheres, as sketched in Fig. 2. A spacecraft attempting to land on Earth from Low Earth Orbit (LEO), or from an interplanetary trajectory, must lose entirely the kinetic energy of its motion relative to the Earth surface. A small fraction of this energy can be exchanged for potential energy in space by deboosting maneuvers carried out with retro-rockets to decrease the orbital altitude and place the spacecraft on a trajectory intercepting the Earth surface. However, utilization of retro-rockets for the entire maneuver until touchdown is unfeasible because of the exceedingly large weight of propellant that would have to be carried onboard. It is therefore the atmosphere and the aero-braking force it exerts on the spacecraft that are responsible for dissipating more than 99% of the orbital kinetic energy. Orbital kinetic energies correspond to entry velocities U_E involving very high Mach numbers across the fringe of the atmosphere, as discussed below. These high velocities persist for a large portion of the trajectory in the atmosphere and greatly complicate the calculation of thermomechanical loads on the spacecraft. Unless means of teleporting crews and equipment from orbit to the surface of planets are ever discovered, it is likely that Hypersonics will remain a problem that all future generations of engineers will have to address in the design of planetary landing systems for as long as mankind pursues exploration of space.

The fringe of the atmosphere, or the edge of space, is a rather blurry boundary where the atmosphere density is sufficiently low such that the aerodynamic forces above that altitude are negligible. There are several definitions of this boundary, but one commonly used is the *"von Kármán line"*, approximately located at an altitude of $z_{\rm E} = 91$ km above the Earth surface. For $z > z_{\rm E}$, the motion of the spacecraft is described by Orbital Mechanics. The domain of Hypersonics begins where the vacuum of space terminates, since the presence of an atmosphere and the force it creates against the moving body is imperative for observation of the distinguished flow phenomena discussed here. As the flight altitude of the spacecraft decreases below the entry interface $z = z_{\rm E}$, the hypersonic aerodynamic forces become increasingly important, whereas the Kepler force that balances gravity in orbital motion becomes irrelevant. Consequently, because of the effect of the atmosphere, the spacecraft trajectory deviates from the vacuum conic predicted by Orbital Mechanics. The friction forces created by the atmosphere lead to high heating rates of the fuselage, with peak heating values typically occurring well below the entry interface at altitudes of order unity when nondimensionalized with the planetary scale height, where the density is not too low and the flight speed is still hypersonic.

To quantify the characteristic velocities participating in re-entry applications of Hypersonics, it is convenient to recall here some elementary concepts of Orbital Mechanics. Consider the fundamental result of the classical central-force problem whereby the specific mechanical energy of an object orbiting at a velocity v and distance r from the center of a planet,

$$\mathscr{E} = \frac{\mathrm{v}^2}{2} - \frac{\mu}{r} = C, \tag{2}$$

must remain equal to a constant C during its motion, where $\mu = GM$ is the standard gravitational parameter based on the universal gravitational constant $G = 6.67 \cdot 10^{-11}$ m^3/kgs^2 and on the mass M of the planet. Equation (2) states that the orbiting body cannot lose or gain mechanical energy, but it can only exchange kinetic energy for potential energy. By solving the equation of motion of the orbiting body in the radial direction, it can be shown that the trajectory followed by the body must be a conic one, and that the constant C in Eq. (2) is equal to

$$C = -\mu(1-e)/(2r_p), \tag{3}$$

where e is the orbit eccentricity and r_p is the periapsis radius, or equivalently, the minimum radial distance of approach measured from the center of the planet. Upon substituting Eq. (3) into Eq. (2), the expression

$$\mathrm{v} = \sqrt{2\mu\left(\frac{1}{r} - \frac{1-e}{2r_p}\right)} \tag{4}$$

is obtained for the orbital velocity of the spacecraft as a function of the radial distance r.

For circular orbits ($r_p = r$ and $e = 0$), Eq. (4) becomes the circular orbital velocity

$$\mathrm{v_O} = \sqrt{\mu/r}, \tag{5}$$

which varies inversely with the radius of the orbit. For spacecrafts orbiting at small altitudes $z = r - R$ compared to the radius of the planet R, Eq. (5) can be expanded in Taylor series as $\mathrm{v_O} \approx \mathrm{v_{C1}}\left[1 - (z/2R) + O\left(z/R\right)^2\right]$ thereby indicating that $\mathrm{v_O}$ is equal to $\mathrm{v_{C1}}$ in the first approximation, where $\mathrm{v_{C1}}$ is referred to as the *"first cosmic velocity"* and is defined as

$$\mathrm{v_{C1}} = \sqrt{\mu/R} = \sqrt{g_0 R}. \tag{6}$$

In Eq. (6), g_0 is the value of the gravitational acceleration $g = \mu/r^2$ on the surface of the planet $r = R$.

Velocities larger than (5) lead to supercircular (elliptic, parabolic, and hyperbolic) orbits. A limiting case corresponds to that of parabolic orbits, $e = 1$, for which the kinetic and potential energies are equal everywhere along the orbit. In this case, Eq. (4) becomes the escape velocity

$$\mathrm{v_{ESC}} = \sqrt{2\mu/r}. \tag{7}$$

The escape velocity $\mathrm{v_{ESC}}$ attains its maximum value at the periapsis of the parabolic orbit $r = r_p$, and it vanishes far away at $r \to \infty$. In this way, $\sqrt{2\mu/r_p}$ is both the minimum velocity necessary to initiate a escape maneuver from the gravitational field of the planet, and the minimum arrival velocity from a parabolic trajectory at the periapsis. Similarly to the analysis above, Eq. (7) may be expanded in Taylor series as $\mathrm{v_{ESC}} \approx \mathrm{v_{C2}}\left[1 - (z_p/2R) + O\left(z_p/R\right)^2\right]$, around the periapsis altitude $z_p = r_p - R$ for $z_p/R \ll 1$, thereby indicating that $\mathrm{v_{ESC}}$ is equal to $\mathrm{v_{C2}}$ in the first approximation at the periapsis. In this formulation, $\mathrm{v_{C2}}$ is referred to as the *"second cosmic velocity"* and is defined as

$$\mathrm{v_{C2}} = \sqrt{2\mu/R} = \sqrt{2g_0 R}. \tag{8}$$

The relevance of the velocity scales $\mathrm{v_{C1}}$ and $\mathrm{v_{C2}}$ rests on the following considerations.

	Venus ♀	Earth ⊕	Mars ♂	Jupiter ♃	Saturn ♄	Uranus ⛢	Neptune Ψ	Titan (Saturn's moon)
R [km]	6,100	6,371	3,415	71,375	60,500	24,850	25,000	2,575
g_0 [m/s^2]	8.8	9.8	3.7	24.3	10.0	9.4	10.9	1.3
v_{C1} [km/s]	7.3	7.9	3.5	41.6	24.6	15.3	16.5	1.8
v_{C2} [km/s]	10.4	11.1	5.0	58.9	34.8	21.6	23.3	2.6
$\mathrm{v}_{\mathrm{HEX},\oplus}$ [km/s]	2.5	–	2.9	8.8	10.2	11.3	11.6	11.6
v_{ω} [km/s]	0.002	0.465	0.240	12.6	9.9	4.2	2.7	0.012

Table 1: Radius R, surface gravity g_0, cosmic velocities v_{C1} and v_{C2}, hyperbolic excess velocity $\mathrm{v}_{\mathrm{HEX},\oplus}$ at arrival to Earth, and the equatorial rotation velocity v_{ω} of selected celestial bodies.

The ratio of the orbit altitude z and the radius of the Earth $R_{\oplus}$ is small for spacecrafts in LEO (e.g., $z/R_{\oplus} \approx 0.06$ for the International Space Station). Even smaller is the corresponding ratio based on the altitude of the von Kármán line $z_{\mathrm{E}}/R_{\oplus} = 0.01$, which is similar to the ratio between the thickness of the skin of an apple and its size. As a result, the velocities participating in the re-entry of spacecrafts from circular LEO are of the same order as the first cosmic velocity,

$$U_{\mathrm{E}} \approx \mathrm{v}_{\mathrm{C1},\oplus} = 7.9\,\mathrm{km/s}\,, \tag{9}$$

which corresponds to a free-stream Mach number

$$Ma_{\infty} = \mathrm{v}_{\mathrm{C1},\oplus}/a_{\infty} \approx 28 \tag{10}$$

based on the speed of sound $a_{\infty} = 275$ m/s at the von Kármán line. It is however important to remark that the precise value of U_{E} is the result of a deboost maneuver responsible for deorbiting the spacecraft from circular motion and sending it into a descending elliptic orbit intercepting the entry interface, as sketched in Fig. 3. It can be shown that $(U_{\mathrm{E}} - \mathrm{v}_{\mathrm{C1},\oplus})/\mathrm{v}_{\mathrm{C1},\oplus}$ is a small quantity of order $z_{\mathrm{E}}/R_{\oplus} \ll 1$ in practical deboost maneuvers, where the entry angle γ_{E} is small.

A case where (9) is also a good approximation for U_{E} is the re-entry of nose cones of intercontinental ballistic missiles (ICBMs). As depicted in Fig. 3, the trajectory followed by ICBMs is mostly an elliptical one that intercepts the Earth's surface at the impact point, with the apogee being located at relatively high altitudes of order $1,000 - 1,500$ km. Typical altitudes at the burnout point during ascent, where the fuel is exhausted and the missile begins coasting along a Keplerian ellipse, are $z_{\mathrm{BO}} \approx 150 - 400$ km. The corresponding burnout velocities v_{BO} are large fractions of the circular orbital velocity (5) at the burnout altitude. For instance, the burnout velocity of the LGM-30 Minuteman-III missile is $\mathrm{v}_{\mathrm{BO}} \approx 6.7$ km/s at $z_{\mathrm{BO}} \approx 190$ km, or equivalently, 85% of the circular velocity v_{O} at that altitude. For burnout

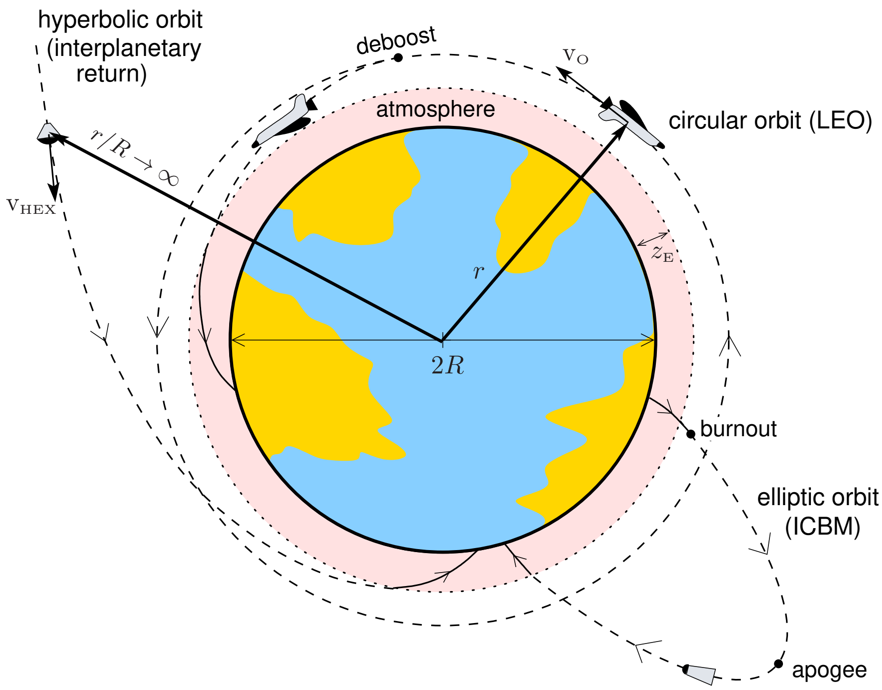

Figure 3: Schematics of circular, hyperbolic, and elliptic orbits utilized, respectively, by LEO spacecrafts, interplanetary return capsules, and intercontinental ballistic missiles.

altitudes not too far from the edge of space, the entry velocity U_E is similar to $\mathrm{v_{BO}}$ because of the approximate symmetry of the elliptical orbit. As a result, since $z_\mathrm{BO}/R_\oplus \ll 1$, the entry velocity U_E is similar to $\mathrm{v_{C1}}$ in most practical scenarios. The entry angle γ_E is however much larger for ICBMs than for spacecrafts re-entering from LEO because of the necessary minimization of the time to impact in order to avoid interception by enemy countermeasures.

Atmospheric re-entry of spacecrafts returning from interplanetary missions in the Solar System is a significantly less frequent event than from LEO. With exception of the Apollo and USSR's Luna missions to the Moon, and a few sample-return missions from asteroids and Phobos, the entry of objects in the terrestrial atmosphere coming from outer space has been reserved in history for meteoroids on heliocentric and interstellar orbits intercepting the Earth's orbit. For those, the approach to the boundary of the Earth's sphere of gravitational influence (located approximately at $100R_\oplus$ from the Earth's center) occurs along a hyperbolic orbit intercepting the entry interface. To survive the high heating rates during re-entry, or to avoid skipping on the atmosphere and being deflected into space, the re-entering object must intercept the atmosphere within an appropriate range of altitudes commonly referred to as the *"re-entry corridor"*.

In the simplest form of hypothetical arrival of a spacecraft from another planet in the Solar System, namely that originated from a heliocentric Hohmann transfer, the spacecraft would cross the boundary of the Earth's sphere of gravitational influence at a hyperbolic excess velocity $\mathrm{v}_{\mathrm{HEX},\oplus}$ given by the absolute value of the difference between the Earth's orbital speed around the Sun (29.8 km/s) and the velocity at the aphelium (for arrivals from planets closer to the Sun than Earth) or perihelium (for arrivals from planets farther from the Sun than Earth) of the Hohmann ellipse. Characteristic values of $\mathrm{v}_{\mathrm{HEX},\oplus}$ are provided in Table 1, whereas the details of the calculations are skipped here, since they are more appropriate for textbooks focused on Orbital Mechanics. Given $\mathrm{v}_{\mathrm{HEX},\oplus}$, the entry velocity U_{E} can be calculated utilizing the conservation of energy (2) along the hyperbolic orbit from far away from Earth, $r/R_\oplus \to \infty$, to the entry interface $r = z_{\mathrm{E}} + R_\oplus$, thereby giving

$$\frac{\mathrm{v}^2_{\mathrm{HEX},\oplus}}{2} = \frac{U^2_{\mathrm{E}}}{2} - \frac{\mu_\oplus}{z_{\mathrm{E}} + R_\oplus}, \tag{11}$$

where the second term on the right-hand side corresponds to the escape kinetic energy $\mathrm{v}^2_{\mathrm{ESC}}/2$ at the entry interface. Utilizing the approximation $z_{\mathrm{E}}/R_\oplus \ll 1$ in Eq. (11), along with the definition (8), the expression

$$U_{\mathrm{E}} \approx \sqrt{\mathrm{v}^2_{\mathrm{HEX},\oplus} + \mathrm{v}^2_{\mathrm{C2},\oplus}} \tag{12}$$

is obtained for the entry velocity to leading order in $z_{\mathrm{E}}/R_\oplus$. Return missions from our nearest neighbors Venus and Mars require values of $\mathrm{v}_{\mathrm{HEX},\oplus}$ relatively small compared to the second cosmic velocity $\mathrm{v}_{\mathrm{C2},\oplus}$. For those, the entry velocity (12) can be approximated as

$$U_{\mathrm{E}} \approx \mathrm{v}_{\mathrm{C2},\oplus} = 11.1\,\mathrm{km/s}\,, \tag{13}$$

which corresponds to a free-stream Mach number

$$Ma_\infty = \mathrm{v}_{\mathrm{C2},\oplus}/a_\infty \approx 40 \tag{14}$$

at the von Kármán line. Return missions from any of the outer planets require values of $\mathrm{v}_{\mathrm{HEX},\oplus}$ comparable or larger than $\mathrm{v}_{\mathrm{C2},\oplus}$, and give rise to entry Mach numbers as large as

$$Ma_\infty = \left(\sqrt{\mathrm{v}^2_{\mathrm{HEX},\oplus} + \mathrm{v}^2_{\mathrm{C2},\oplus}}\right)/a_\infty \approx 58 \tag{15}$$

for a return from Neptune and based on speed of sound at the von Kármán line.

Because of the strongly binary character of the Earth/Moon system, the orbital description of Lunar returns is not as simple as the computation of interplanetary Hohmann transfers, and requires further considerations involving patched Keplerian conics that are beyond the scope of these notes. However, the participating entry velocities at arrival to Earth U_{E} are also of the same order as the second cosmic velocity $\mathrm{v}_{\mathrm{C2},\oplus}$, as in Eq. (13).

As shown in Table 1, massive outer planets such as Jupiter have very large values of v_{C1}

and v_{C2}. Spacecrafts entering in the atmospheres of those planets will experience correspondingly high levels of acceleration and heating. Also shown in Table 1 is that both v_{C1} and v_{C2} are much larger than the rotation velocity at the equator v_ω of inner planets, including Earth, along with Saturn's moon Titan. Consequently, for those celestial bodies, entering from either direct orbits offers little advantage over entering from retrograde orbits, since both yield mostly the same relative motion between the spacecraft and the atmosphere.

The considerations above illustrate the high Mach numbers attained during atmospheric re-entry. However, a question that often arises among students of Hypersonics is: *"why is the Hypersonics literature focused on the problem of re-entering the atmosphere and not so much on the problem of exiting it?"*. It should be stressed that rocket-powered spacecrafts, in their ascent to LEO, routinely reach hypersonic Mach numbers $Ma_\infty \sim 5-12$ within the atmosphere, although they are never as large as those involved in re-entry. During ascent, most of the positive velocity differential Δv required for attaining orbital kinetic energies is provided by the upper stages of the rocket at altitudes far above the fringe of the atmosphere. The rationale for this is evident, in that it takes full advantage of rocket propulsion in space, and minimizes friction and fuel consumption while the spacecraft ascends in the atmosphere. In contrast, the large negative Δv required to stop the spacecraft from orbital to zero velocity, corresponding to a variation of the Mach number from $Ma_\infty \gtrsim 28$ to zero, is attained entirely within the atmosphere during re-entry, thereby creating much more pressing problems of acceleration and heating than during ascent to orbit.

3. The heat barrier

The flow pattern around hypersonic flight systems changes significantly in applications involving acceleration from takeoff speed to cruise speeds, as depicted in Fig. 4 for the case of a slender body. At subsonic speeds ($Ma_\infty \ll 1$), the pressure field is elliptic, and consequently, the streamlines become deflected far upstream by the presence of the body. In transonic conditions ($Ma_\infty \lesssim 1$), the acceleration of the flow caused by the favorable pressure gradients along the sides of the body lead to locally sonic and supersonic flow in spite of the subsonic flow prevailing upstream. The shock caused by transonic conditions oftentimes causes boundary-layer separation and a large increase in drag, and its deleterious effects on control surfaces represents a primary concern for the maneuverability of aircrafts breaking the sound barrier. As the Mach number is increased, the compression shock moves downstream whereas the sonic line moves upstream, the latter eventually becoming a bow shock when the free stream is supersonic, $Ma_\infty > 1$. Further increase in the Mach number involves weakening the shock waves, which become increasingly oblique to the flow.

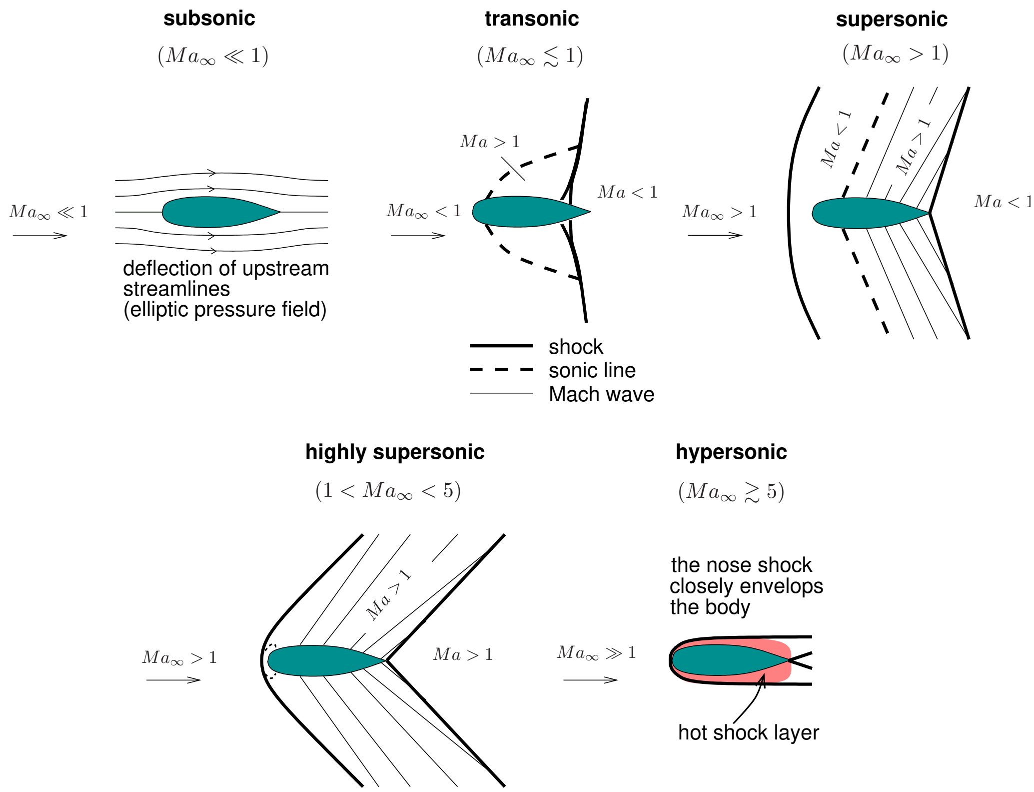

Figure 4: Flow pattern around a slender body as Ma_∞ increases.

At hypersonic velocities ($Ma_\infty \gtrsim 5$), the nose shock closely envelops the surface of the body and leads to a hot shock layer whose thermomechanical effects can be devastating for the structural integrity of the fuselage. The realm of hypersonics is not one associated with the onset of compressibility effects such as those encountered when transitioning from subsonic to supersonic flight. Those effects are the focus of transonic and low-supersonic aerodynamics, and their challenges were greatly overcome by the breaking of the sound barrier in 1947. Instead, the problem of hypersonics is related to the ever-increasing heat barrier that is encountered by the flight system as its Mach number is increased above approximately 5.

Figure 5 provides velocity-altitude trajectories for different hypersonic flight systems that illustrate the range of velocities described in Sections 1 and 2. In interpreting the curves, it is important to note that flight speeds U_∞ expressed in kft/s are numerically equivalent to the flight Mach number Ma_∞ at 35 km of altitude in the stratosphere, where the speed of sound becomes $a_\infty \sim 1$ kft/s. Figure 5 is referred to throughout the remainder of the text in connection with multiple concepts. For now, it suffices to mention that the current state-of-the-art in hypersonic technology prevents hypersonic systems from venturing into the range of the diagram corresponding to high Mach numbers at low altitudes in continuous-

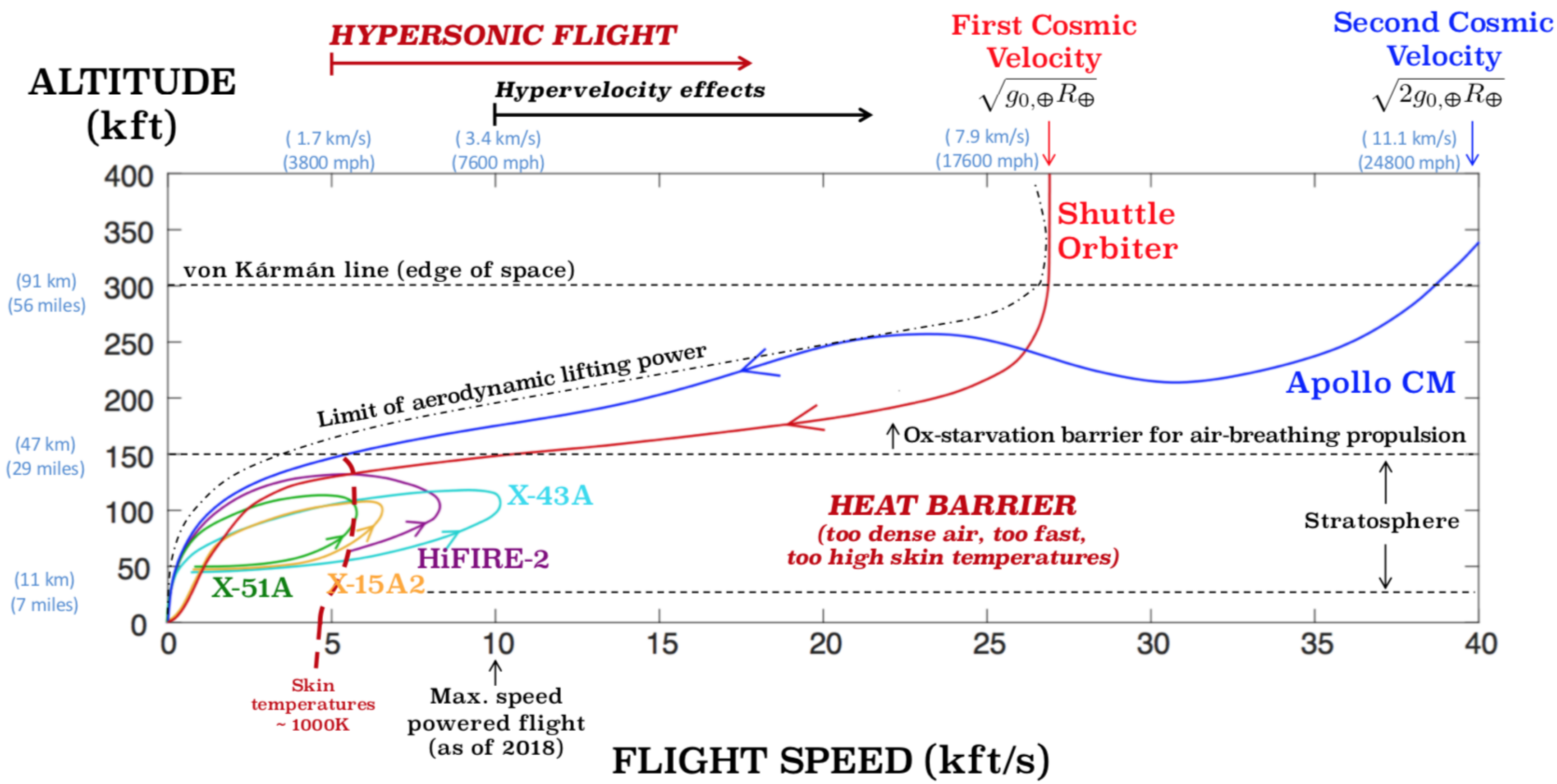

Figure 5: Velocity-altitude trajectories for different hypersonic flight systems.

level flight, where the heat barrier hinders further progress. This prohibited range, which is deliberately avoided by all existing flight trajectories of man-made objects, involves high enthalpies, high Mach numbers, and high Reynolds numbers.

In most engineering applications, the specific kinetic energies of the airflow around hypersonic flight systems are of order $U_\infty^2/2 \sim 1 - 80$ MJ/kg. These kinetic energies are comparable to or larger than the specific heats of vaporization of water (2.3 MJ/kg), carbon (60 MJ/kg), silica (5.8 MJ/kg), and iron (7.0 MJ/kg), and they are much higher than the specific enthalpy of air at normal conditions (300 kJ/kg). The largeness of the kinetic energy in hypersonic flows is perhaps the root cause of the emergence of the heat barrier, and poses severe challenges in the structural design of fuselages and airframes utilized for hypersonic flight systems, as explained below.

That the kinetic energy in hypersonic flows is large compared to the thermal energy can be understood by noticing that the square of the flight Mach number (1) can be written as

$$Ma_\infty^2 = \frac{2}{\gamma - 1}\left(\frac{U_\infty^2/2}{h_\infty}\right) \tag{16}$$

for a calorically perfect gas with an adiabatic coefficient γ. In this formulation, h_∞ is the static enthalpy of the gas environment,

$$h_\infty = c_p T_\infty, \tag{17}$$

where c_p is the specific heat at constant pressure. As a result, at high Mach numbers, $Ma_\infty^2 \gg 1$, the specific kinetic energy of the free stream is large compared to the static specific enthalpy. This has profound consequences in the structure of the ensuing flow field, and constitutes the core of the problem of hypersonic aerodynamics. In particular, complex effects, unique to the hypersonic gas environment, are driven by the high temperatures attained as a result of the transformation of kinetic energy into thermal energy.

The transformation of kinetic energy into thermal energy in hypersonic flows takes place ubiquitously downstream of shocks, where the flow is compressed and decelerated, as sketched in Fig. 6(a). This transformation is best illustrated by the relation

$$\underbrace{h_{0,\infty}}_{\substack{\text{stagnation enthalpy}\\ \text{(free stream)}}} = \underbrace{\cancelto{\text{small}}{h_\infty}}_{\substack{\text{static enthalpy}\\ \text{(free stream)}}} + \underbrace{\frac{U_\infty^2}{2}}_{\substack{\text{kinetic energy}\\ \text{(free stream)}}} \approx \underbrace{h_2}_{\substack{\text{static enthalpy}\\ \text{(post-shock)}}} + \underbrace{\cancelto{\text{small}}{\frac{U_2^2}{2}}}_{\substack{\text{kinetic energy}\\ \text{(post-shock)}}}, \tag{18}$$

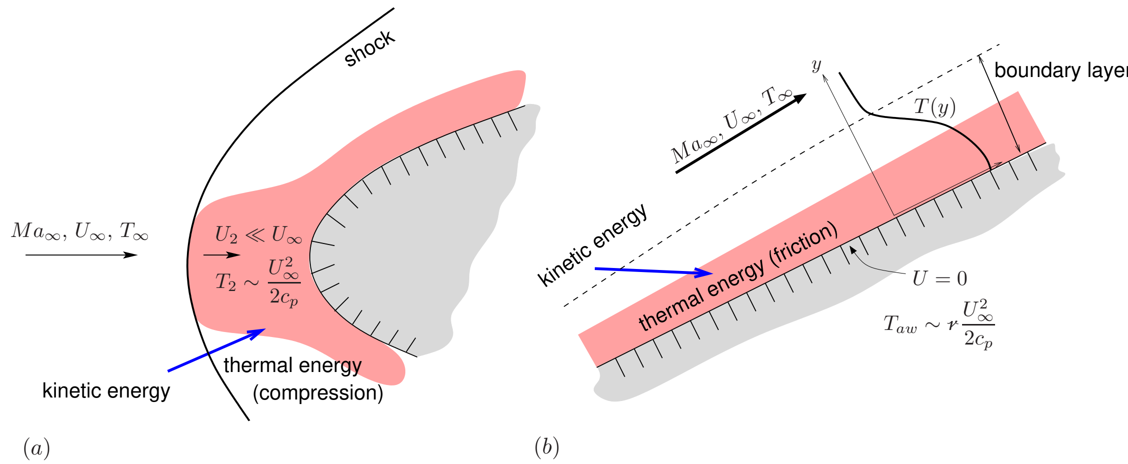

Figure 6: Schematics of hypersonic flows over (a) blunt bodies and (b) flat surfaces.

which represents the well-known result that the stagnation enthalpy is constant across shock waves. At hypersonic Mach numbers, the free-stream static enthalpy and the post-shock kinetic energies become negligible compared, respectively, to the free-stream kinetic energy and the post-shock static enthalpy. The stagnation enthalpy of the free stream is mostly of kinetic origin, $h_{0,\infty} \sim U_\infty^2/2$. Most of the free-stream kinetic energy becomes transformed into local enthalpy in regions where the gas is strongly decelerated, as in the post-shock zone depicted in Fig. 6(a). This leads to a large post-shock temperature of order $T_2 \sim U_\infty^2/(2c_p)$ for calorically perfect gases, with $T_2/T_\infty = O(Ma_\infty^2) \gg 1$. Characteristic values of the true post-shock temperature T_2 in hypersonic flight are $T_2 \sim 3,000$ K for endoatmospheric systems at $Ma_\infty \sim 10$ (e. g., X-43), $T_2 \sim 7,000$ K for re-entry of spacecrafts from LEO at $Ma_\infty \sim 25$ (e. g., Shuttle Orbiter), and $T_2 \sim 11,000$ K for re-entry of spacecrafts from Lunar or interplanetary return trajectories at $Ma_\infty \sim 40$ (e. g., Apollo Command Module). At Mach numbers of 20 and above, the gas downstream of the bow shock emerging from the nose of the spacecraft is very hot and may radiate heat to the fuselage.

The above considerations about kinetic-to-thermal energy conversion also apply qualitatively to hypersonic boundary layers, although the mechanism of energy transformation is fundamentally different. Near the wall, the effect of friction, caused by the necessary compliance with the non-slip boundary condition, leads to an increase in temperature up to values as large as the so-called *"adiabatic wall temperature"* T_{aw}, as sketched in Fig. 6(b). The adiabatic wall temperature T_{aw} is the equilibrium temperature attained by a non-radiative insulated wall in the presence of an overriding hypersonic stream, and is of the same order as $r U_\infty^2/(2c_p) \sim r(\gamma-1)Ma_\infty^2 T_\infty/2 \gg T_\infty$ at high Mach numbers, with $r \lesssim$ being a recovery factor. Hypersonic boundary layers tend to be thicker and hotter than their low-speed counterparts. As a result of the high temperatures, chemical reactions can occur in boundary layers that lead to dissociation and ionization of the air, and to catalysis or recombination of atomic gaseous species diffused into surfaces, as depicted in Fig. 1.

In practical scenarios, the high post-shock temperatures and the high adiabatic wall temperatures do not translate into similarly high temperatures of the fuselage skin T_w,. Besides the fact that the wall temperature is always moderated by radiative cooling to the environment, several techniques for moderating wall temperatures have been developed over the years to reject the intense aerodynamic heating or conveniently absorb it in isolated parts of the structure. These techniques include the utilization of thermal shields based on ablation, heat rejection, heat absorption, and transpiration cooling. The resulting characteristic values of the fuselage skin temperature observed during hypersonic flight are $T_w \sim 1,000$ K for the X-15, $T_w \sim 1,600$ K for the Shuttle Orbiter, and $T_w \sim 2,500$ K for the Apollo Command Module. Note, however, that many of the most important refractory materials and advanced alloys used in high-temperature aerospace applications have melting points similar to some of the fuselage skin temperatures cited above (i.e., $2,750$ K for molybdenum, $2,200$ K for zirconium, $1,700$ K for Inconel-X, or $1,560$ K for beryllium). The high skin temperatures observed in hypersonic flight are to be contrasted with those much lower ones found in supersonic aircraft such as the Concorde ($Ma_\infty \sim 2$, $T_w \sim 380$ K) or the SR-71 Blackbird ($Ma_\infty \sim 3.1$, $T_w \sim 600$ K).

As indicated in Fig. 7, the high temperatures generated in hypersonic flows are sufficient to activate complex thermochemical effects in the gas. Non-calorically-perfect effects, whereby c_p is no longer a constant but becomes a function of temperature, are observed to start at relatively low flight speeds. For instance, at temperatures of approximately 800 K, corresponding to post-shock conditions in the stratosphere at $Ma_\infty \sim 4-5$ (i. e., $U_\infty \sim 1,200-1,500$ m/s), the vibrational degrees of freedom are excited and give rise to temperature-dependent specific heats. Dissociation of oxygen and nitrogen molecules arises at higher speeds whose values depend on the flight altitude. At normal pressure, molecular oxygen begins to dissociate following the reaction $O_2 \rightarrow 2O$ at $T \sim 2,000$ K, while molecular nitrogen begins to dissociate following the reaction $N_2 \rightarrow 2N$ at much higher temperatures, $T \sim 4,000$ K. At $T \sim 9,000$ K, all the air is virtually dissociated into atomic nitrogen and oxygen. These chemical changes have profound effects on the post-shock density that are crucial for the computation of temperatures in hypersonic flows. In the stratosphere, the onset of dissociation begins at $Ma_\infty \sim 7$ (for O_2) and $Ma_\infty \sim 15$ (for N_2), as depicted in Fig. 7. Air ionization begins at $T \sim 9,000$ K at normal pressures following reactions of the type $N \rightarrow N^+ + e^-$ and $O \rightarrow O^+ + e^-$. The characteristic flight Mach number in the stratosphere that delimits where ionization effects begin to be important is $Ma_\infty \sim 25$. Air ionization produces a plasma sheath of weakly ionized gas around the hypersonic vehicle that can cause

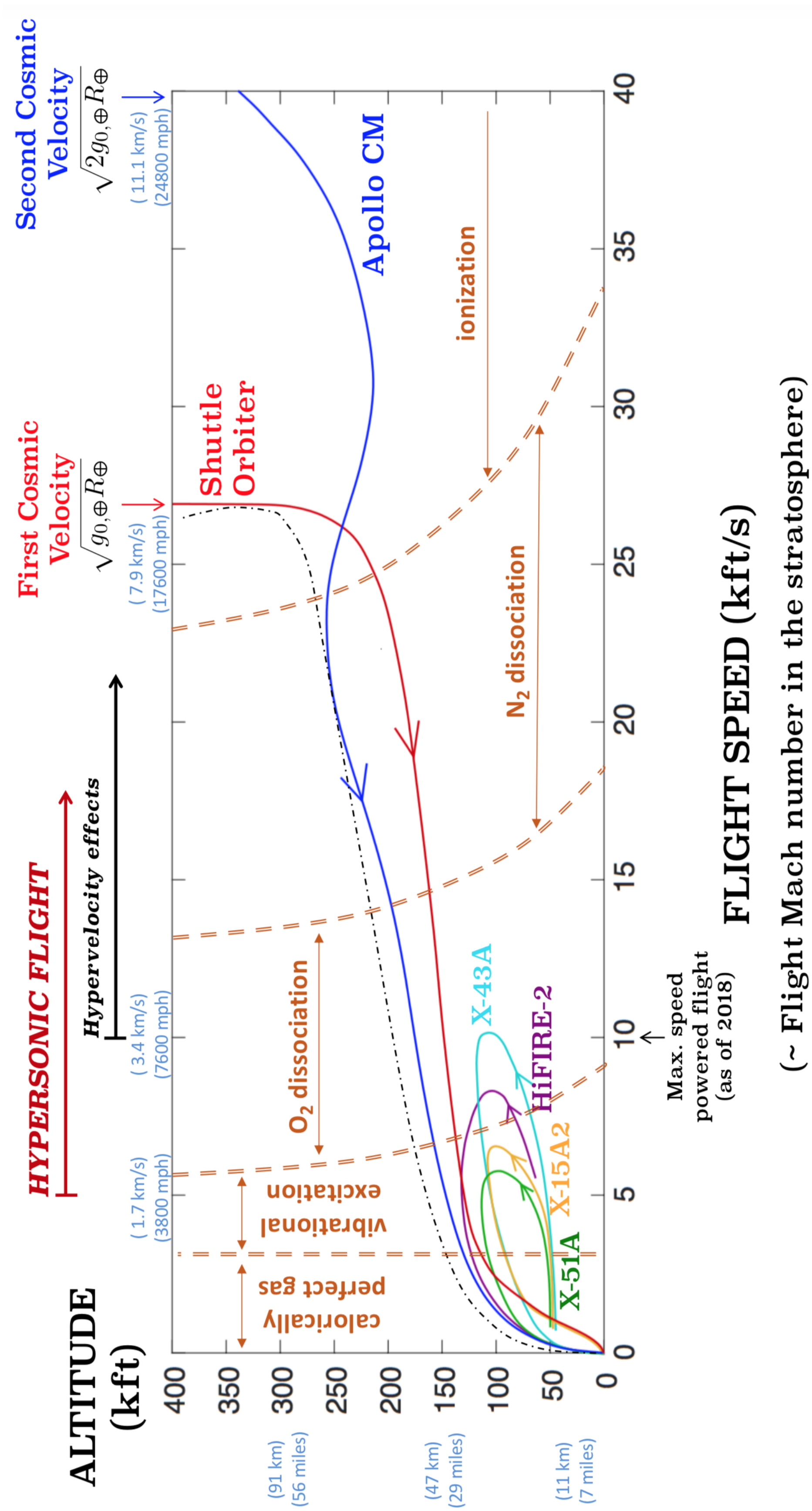

Figure 7: Continuation of the velocity-altitude diagram in Fig. 5.

a communications blackout during a significant portion of the flight, as sketched in Fig. 1. The rates of air dissociation and ionization increase with decreasing pressures, or equivalently, with increasing altitudes. In addition to the aforementioned effects, thermodynamic and chemical non-equilibrium phenomena can occur at high speeds and high altitudes, when the characteristic flow time around the hypersonic vehicle is of the same order or smaller than the time required by molecular collisions to maintain equilibrium.

The intense thermal loads involved in hypersonic flight make necessary the utilization of thermal shields. In choosing a thermal shield, the maximum heat flux $q''_{w,\max}$ imposes the type of material, while the total heat load $Q = \int\int q''_w dS dt$, defined as the double integral of the heat flux with respect to time and wetted surface S, imposes the volume of material. The requirements of the thermal shield are fundamentally different depending on the particular application. Inverse proportionality rules exist between the bluntness of the elements of the vehicle fuselage and the values of q_w and Q. These relations were provided by the study of Allen and Eggers [4]. The main practical consequences of these rules can be observed in the heating profiles sketched in Fig. 8, which illustrate the trends of heat fluxes entering three hypersonic flight systems as a function of the entry time. Nose cones of ICBMs, which have a slender shape, are subject to very high heat fluxes q''_w but for a short amount of time (∼1 min), thereby rendering relatively small values of Q. The preferred thermal shields for these systems consist of thin ablators of carbonaceous materials that gasify rapidly during the short flight times. In contrast, manned spacecrafts are much more blunt, and are consequently subject to much smaller heat fluxes q''_w ($\sim 1/100$ smaller than nose cones of ICBMs) but for a much longer duration (~ 10 mins) because of the necessity of minimizing deceleration, thereby leading to larger values of Q. The thermal shields for these vehicles involve insulating honeycombs of foams or ceramics in conjunction with bulky ablators of carbonaceous materials.

To illustrate the considerations above, consider the re-entry of the Shuttle Orbiter (mass $m \approx 10^5$ kg) orbiting around the Earth at an altitude of $h \approx 350$ km at an orbital velocity similar to the first cosmic velocity (6). During re-entry, the variation of the mechanical energy of the Shuttle Orbiter $\Delta E \approx m v^2_{\mathrm{C1},\oplus}/2 + m g_{0,\oplus} h = 3.3$ TJ is transformed into heat. Note that the variation of potential energy is much smaller (smaller by a factor $h/R_\oplus = 0.05$) than the variation of kinetic energy during re-entry. Since the average consumption of gas and electricity for a typical home in Northern California is 2.5 kWh/day = 9.0 MJ/day, all the heat generated during the re-entry of the Shuttle Orbiter could be used for heating and cooking in a single-person home for 360,000 days, or equivalently, $1,000$ years. However, only a fraction smaller than < 1 % of this heat is transferred to the spacecraft structure, whereas the rest is dissipated in the surrounding air. The particular value of this fraction

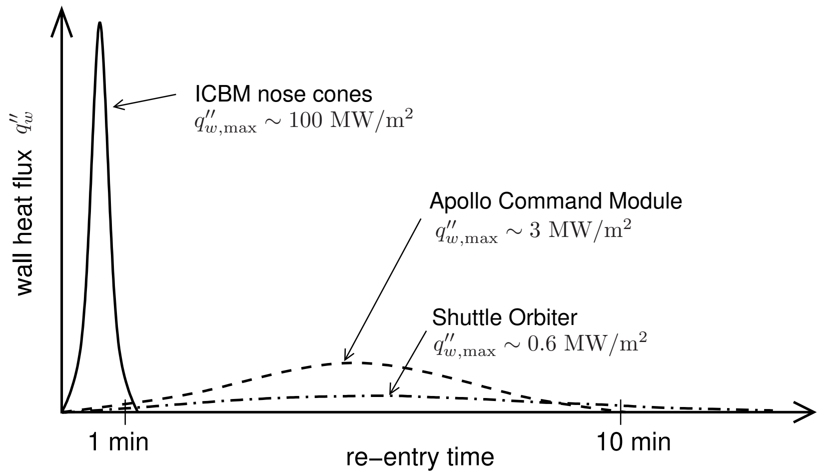

Figure 8: Schematics of the temporal evolution of the wall heat flux during re-entry.

is a solution of the fluid-mechanical problem of atmospheric re-entry, and can be estimated using the theory of Allen and Eggers [4] as

$$\frac{Q}{\Delta E} \approx \frac{C_f S}{2 C_D A}, \tag{19}$$

where C_f is the mean friction coefficient, A is the frontal area, and C_D is the wave drag coefficient of the spacecraft. This estimate establishes that blunt bodies such as space capsules (order-unity C_D and large A) with comparatively low skin friction ($C_f/C_D \ll 1$) and small wetted areas [$S/A = O(1)$], are the most practical for re-entry applications because such aerodynamic shapes enable maximum dissipation of energy in the form of heat into the gas environment (rather than into the spacecraft structure). As the bluntness increases, however, the drag force increases, and the re-entry becomes comparatively slower, thereby leading to a longer time exposure to the scorching heat.

References

[1] Th. von Kármán. Aerodynamic heating. In *Proceedings of the symposium on "High temperature–a tool for the future", Berkeley, California*, 1956.

[2] H. S. Tsien. Similarity laws of hypersonic flows. *MIT J. Math. Phys.*, 25:247–251, 1946.

[3] M. D. van Dyke. The combined supersonic-hypersonic similarity rule. *J. Aeronaut. Sci.*, 18:499–500, 1951.

[4] J. Allen and A. J. Eggers. A study of the motion and aerodynamic heating of ballistic missiles entering the earth's atmosphere at high supersonic speeds. Technical report, NACA TR 1381, 1958.